JPRAS Open 38 (2023) 173–185

Contents lists available at ScienceDirect

JPRAS Open

journal homepage: www.elsevier.com/locate/jpra

Original Article

Positive effects of hypoxic preconditioning of the extracellular matrix and stromal vascular fraction from adipose tissue

Béatrice Dirat[a], Valérie Samouillan[b], Jany Dandurand[b], Jean-Pierre Gardou[c], Valérie Walter[d], Véronique Santran[a,*]

[a] SYMBIOKEN, 42 avenue du Général de Croutte, 31100 Toulouse, France
[b] PHYPOL, CIRIMAT, Institut Carnot Chimie Balard CIRIMAT, Université de Toulouse, Université Paul Sabatier, 118 route de Narbonne, 31062 Toulouse, France
[c] LAPLACE, Université de Toulouse, CNRS, INPT, Université Paul Sabatier, 118 route de Narbonne, 31062 Toulouse, France
[d] Department of Plastic and Reconstructive Surgery, Clinique la Croix du Sud, 31130 Quint Fonsegrive, France

ARTICLE INFO

Article history:
Received 20 April 2023
Accepted 23 September 2023
Available online 30 September 2023

Keywords:
Hypoxia
SVF
Stem cells
Extracellular matrix
Collagen

ABSTRACT

Background: Numerous approaches have been developed to decelerate the aging process of facial skin. Synthetic fillers and cell-enriched fat grafts are the main procedures employed to fill wrinkles.
Objective: The aim of this study was to evaluate the *in vitro* and *in vivo* safety and efficiency of a new process developed by SYMBIOKEN: the AmeaCell, which facilitates the extraction of the stromal vascular fraction (SVF) and the associated hypoxia pre-conditioned matrix to promote fat graft survival.
Methods: The AmeaCell device allows the extraction from adipose tissue of SVF and pre-conditioned MatriCS and promotes a hypoxic environment. Experiments were carried out on human cells and then in mice.
Results: Characterization of cells and MatriCS showed that after their extraction using the new process developed by SYMBIOKEN, the extracted cells expressed stem-cell markers. The presence of characteristic proteins and lipid fractions found in the adipose matrix were confirmed in MatriCS. Cobalt chloride treatment of the matrix using the AmeaCell device induced modifications in the ma-

* Corresponding author.
E-mail address: veronique.santran@symbioken.com (V. Santran).

https://doi.org/10.1016/j.jpra.2023.09.007

trix composition with a decrease in laminin and without collagen modification, both of which promote adhesion and differentiation of SVF or adipose-derived stromal cells. The combination of MatriCS and SVF (1×10^6 and 5×10^6, respectively) is safe and efficient to fill wrinkles induced by UVB irradiation. The cross-talk between MatriCS and SVF can act a durable filler compared to the filling performed using cells or matrix or fat alone, which need to be replaced frequently.

Conclusion: These results indicate that the combination of MatriCS and SVF is safe and effective as a biological filler for achieving skin rejuvenation and wrinkle filling.

Introduction

During aging, degenerative processes affect the skin and deep structures of the face, such as loss of collagen, elastin, and reticulin fibers, leading to the appearance of wrinkles.[1] Many approaches have been developed to decelerate the process of facial skin aging. One of them is the use of synthetic injectable fillers, such as hyaluronic acid products, which are biocompatible and have different mechanical properties. These filling agents primarily compensate for volume loss, but do not biologically rejuvenate the skin[2] and need to be replaced frequently.[3]

Autologous fat grafting is another option to biologically rejuvenate the skin.[4] To overcome the high rates of resorption, ranging from 20 % to 80 %, and increase its survival, enrichment of fat graft with cells can be performed.[5–7] Cells can be adipose-derived stromal cells (ADSCs) or stromal vascular fraction (SVF)-derived cells composed of multipotent cells, including ADSCs, fibroblasts, immune and endothelial cells, and pericytes.[8] Several publications have demonstrated the positive outcomes of cell-enriched fat graft in improving facial skin quality (owing to the secretion of growth factors and neovascularization) and its promising potential for application in clinical settings.[8–10]

AmeaCell®, developed by SYMBIOKEN, allows the extraction of SVF and its associated preconditioned matrix from adipose tissue. The partially decellularized matrix is incubated with cobalt chloride solution to promote hypoxia. Hypoxia is known to up regulate the proliferation, differentiation, adhesion, growth factors secretion, and angiogenesis, thereby promoting fat graft survival.[11]

The aim of this study is to evaluate the *in vitro* and *in vivo* safety and efficiency of AmeaCell, which facilitates the extraction of SVF and the associated hypoxia pre-conditioned matrix.

Materials and methods

Isolation of SVF, ADSCs, and MatriCS

Liposuction samples were obtained from healthy patients after acquiring informed consents from them. According to the AmeaCell protocol (not yet commercialized; Figure 1), fat is digested with type I collagenase (Nordmark, Germany) resulting in four phases (Figure 2). The SVF pellet is resuspended in saline buffer and the matrix exposed to cobalt chloride solution (200 µM) (Sigma–Aldrich, France) according to a patented process. This pre-conditioned matrix will be referred to as MatriCS in the rest of the article.

To obtain ADSCs, cells were cultured in Dulbecco's modified Eagle medium (DMEM; Dutscher, France), 10 % fetal bovine serum, 100 units/ml of penicillin, and 100 µg/ml of streptomycin. ADSCs from passages 1 to 2 were used for the experiments.

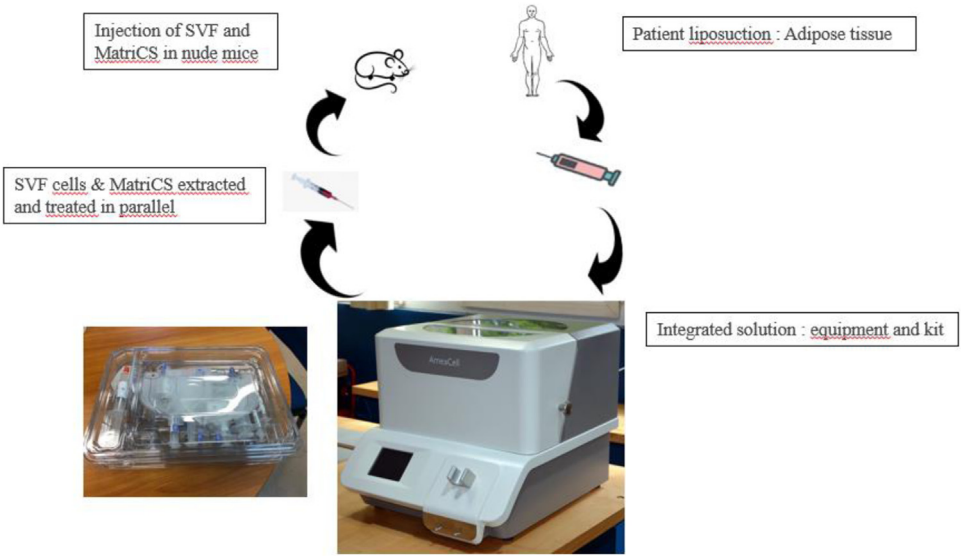

Figure 1. AmeaCell process: liposuction adipose from a patient tissue was transferred into bags of the AmeaCell kit, then into the machine to obtain extracted SVF cells and MatriCS. Both were re-injected into nude mice. A process assistant on the screen of the machine, instructed the operator on the procedure used to treat the two phases using designated elements of the kit. The process followed by the operator is sequential. The operator cannot modify any of the parameters which maintain the repeatability of the process and its success.

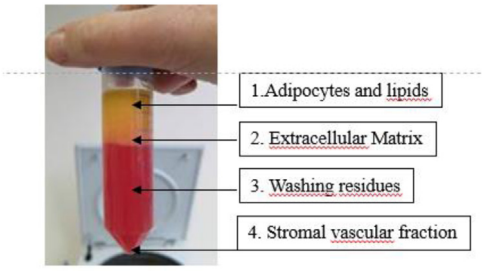

Figure 2. Four phases obtained after collagenase digestion. Phases 1 and 3 were discarded. The extracellular matrix (Phase 2) and SVF cells (Phase 4) were harvested, and processed separately according to the AmeaCell protocol.

Characterization of SVF and MatriCS

Cells were characterized using flow cytometry (FACScalibur Beckton Dickinson, France). They were stained using FITC-coupled CD45 and PE-coupled CD90, CD105, CD31, CD34, and HLA-DR antibodies and appropriate isotypic control (Abcam, France).

Vibrational characterization and thermal analysis of MatriCS

Fourier Transform Infrared Spectroscopy (FTIR)-Attenuated Total Reflectance (ATR) spectra of the freeze-dried matrices were acquired using a Nicolet 5700 FTIR-ATR instrument (Thermo Fisher Scientific, Waltham, MA, USA) in the ATR mode as previously described.[12] For each sample, 64 interferograms were recorded in the 4000–450 cm^{-1} region, co-added and Fourier transformed to generate an average spectrum with a nominal resolution between overlapping bands of 4 cm^{-1}. The single-

beam background spectrum collected from the clean diamond crystal before each experiment was subtracted from the spectra before baseline correction.

Differential scanning calorimetry (DSC) analyses were performed on hydrated samples using a DSC-Pyris calorimeter (Perkin Elmer, Waltham, MA, USA) calibrated as previously described,[12] resulting in a temperature accuracy of 0.1 °C and an enthalpy accuracy of 0.2 J/g.

Fresh samples, 20–25 mg in weight, were equilibrated before cooling to −50 °C at 10 °C/min. The thermograms were recorded during the heating cycle at 10 °C/min until the temperature reached 80 °C.

Cobalt dosage measurement

MatriCS exposed to cobalt chloride solution were subjected to cobalt dosage analysis. Briefly, MatriCS was centrifuged and the phases were separated. Each phase was mineralized independently using nitric and hydrochloric acids and the cobalt content was quantified using ICP/MS (Thermo Scientific, ICAPQ, France).

Animal experiments

All experimental procedures were approved by the US006/CREFRE Ethics committee. Animals were checked daily for signs of inflammation, ulceration, tumor formation, or any negative side effects.

Wrinkle induction: Five-week-old female athymic mice ($n = 5$; Charles River Laboratories, France) were irradiated with UVB dorsally as previously described.[13] After wrinkles induction, SVF (10^5 cells/mice) and MatriCS were prepared and injected into a restricted subcutaneous area. Negative replicas of dorsal skin surface were prepared using a silicon-based impression material (SILFLO, France). Pictures were digitized, and analyzed using Skin Exigence (Besançon, France). The parameters used in the evaluation were depth and volume of the macro-relief. Each replica was analyzed using the Dermatop Blue system (Creative tools, India).

GFP-ADSCs experiment: Six-week old female mice (Crl:NU(lco)-Fox1nu; $n = 3$; Charles River Laboratories, France) were subcutaneously injected with ADSCs (1 or 5×10^6 cells) combined with MatriCS or a nonexposed matrix.

ADSCs transduction: 2×10^6 ADSCs were cultured in a T75-flask and transduced using rLV.EF1.turboGFP viral particles (Vectalys, France) with 4 µg/ml of polybrene (Sigma–Aldrich, France). After 48 h of transduction, cells were checked for Green Fluorescent Protein (GFP) expression using the ZOE fluorescent cell imager (Biorad, France).

Histological analysis

The different matrices obtained from the *in vitro* and *in vivo* experiments were collected and embedded in paraffin for further characterization. Type I and IV collagen (AbCam, France), laminin (Sigma-Aldrich, France), Ki67 (Vector, France), and von Willebrand factor (Dako, France) primary antibodies were used.

For the GFP-ADSCs experiment, the injected skin areas and excised organs were fixed and embedded in optimal cutting temperature (OCT) (Dutscher, France). The fluorescence was visualized using a microscope (DM4000B model, Leica, France)

Results

Characterization of SVF and MatriCS

The FTIR-ATR spectrum of the total fraction (Figure 3A) presented intense and specific absorptions by the lipid fraction, indicating lipids as the major constituents of MatriCS. Weak proteins bands absorptions were also detected in the FTIR-ATR spectrum of MatriCS, at the same position as in the protein fraction spectrum (Figure 3B). The presence of the characteristic collagen feature at 1338, 1280, 1234 and 1202 cm^{-1} [14,15] and the absorption bands of collagen/glycoproteins at 1080 and

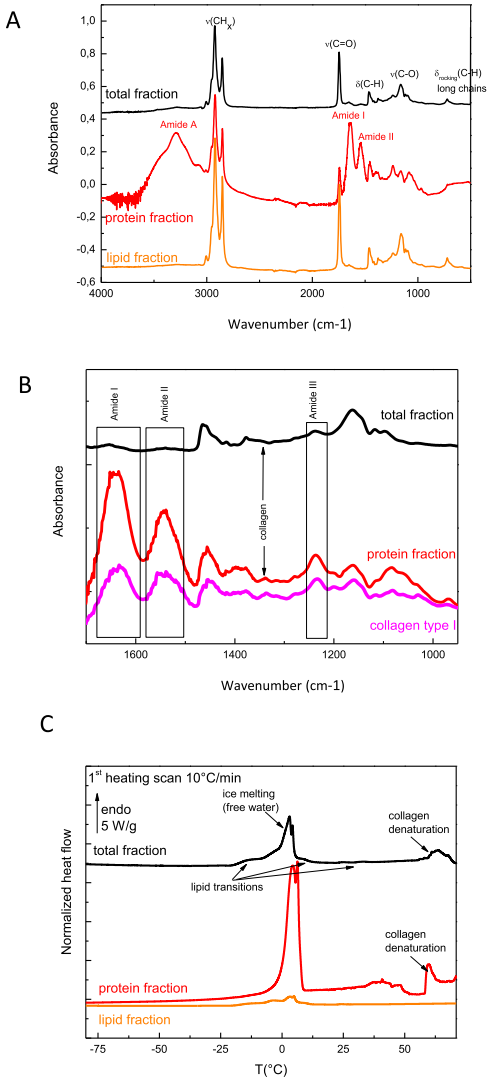

Figure **3**

Figure 3. MatriCS characterization. (A) FTIR-ATR spectra of freeze-dried matrices (total, protein, and lipid fractions) in the 4000–500 cm^{-1} zone indicating that lipids are the major constituents of the total fraction. Band assignment is carried out accordingly.[39,40] (B) FTIR-ATR spectra of freeze-dried matrices and pure collagen type I in the 1700–950 cm^{-1} zone, demonstrating the presence of collagen in the protein and total fractions. (C) DSC thermograms of fresh matrices (total, protein, and lipid fractions) evidencing the thermal signature of water, lipids, and collagen in the total fraction.

1050 cm^{-1} highlight the extracellular matrix (ECM) vibrational signature in MatriCS. The results of DSC (Figure 3C) indicate that MatriCS and protein fraction exhibit the characteristic endotherm of ice melting associated with the presence of freezable water, which is used to estimate the amount of free water.[12] The total amount of water in MatriCS is estimated at 35 ± 6 %, separated into free water (11 ± 3 %) and bound water (24 ± 6 %). The thermal signature of collagen, detected as an endothermic peak in the 60–70 °C range for both the protein fraction and whole matrix, correspond to the collapse of the triple helical structure.[15] From this, it can be inferred that nondenatured collagen is present in

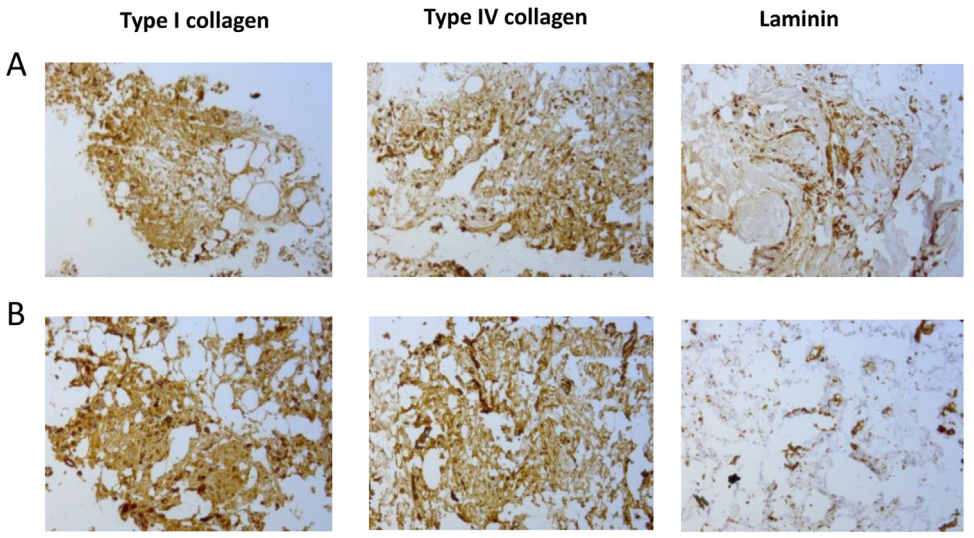

Figure 4. Representative histological staining of MatriCS obtained according to the AmeaCell process (magnification x10). Adipose matrix was exposed (B) or not exposed (A) to cobalt chloride solution. Brown staining can be observed on the section for type I collagen, type IV collagen, and laminin. (For interpretation of the references to color in this figure legend, the reader is referred to the web version of this article.)

MatriCS. The multiple lipids transitions including crystal-liquid and melting[16,17] were detected in the range −20–40 °C for the whole and lipid fractions.

Histological staining (Figure 4) showed that MatriCS expresses ECM components such as type I and IV collagen and laminin. Irrespective of the type of collagen considered, significant changes were not observed, only laminin expression decreased after cobalt chloride exposure.

Flow cytometry analyses showed that SVF is composed of CD34−, CD90+, or CD105+ cells, characteristic of mesenchymal stem cells of adipose tissue, that can differentiate into classical cell lineages such as osteoblastic, adipogenic, and chondroblastic cells.[18] SVF cells include CD34+ or CD31− cells as endothelial progenitors; CD34+ or CD31+ as capillary-forming cells; and CD45+ as markers of lymphocytes (data not shown).

Animal experiments

No adverse events were observed over the period of investigation.

The effect of subcutaneous SVF injection associated with MatriCS on skin rejuvenation was investigated using the wrinkle induction experiment. At 4 weeks post injection, the mice were sacrificed. Histological studies on the skin and replica analysis of wrinkles were performed. In the normal skin group (positive control with no irradiation and no injection), Ki67 staining showed cells in active proliferation at the junction epidermis-dermis. In irradiated mice with no injection (negative control), the thickness of epidermis increased and proliferation at the junction epidermis-dermis was less prominent compared to that in the mice with normal skin. In the test group subjected to skin irradiation and injection with MatriCS + SVF, cell proliferation was more pronounced compared to that in the negative control, and was close to the proliferation observed in the positive control (Figure 5). Collagen was less expressed in the skin of negative control than in normal skin group or the test group. Few capillaries that were stained using the von Willebrand factor, an endothelial cell marker, were also visible in the test group. They appeared to be less numerous than those in the normal skin group, and more than those in the irradiated and untreated skin groups (data not shown).

Analysis of digitized images of replicas in Figure 6 aided in the quantification of the macro-relief. Images showed that the treatment using SVF and MatriCS can significantly reduce the depth of skin wrinkles.

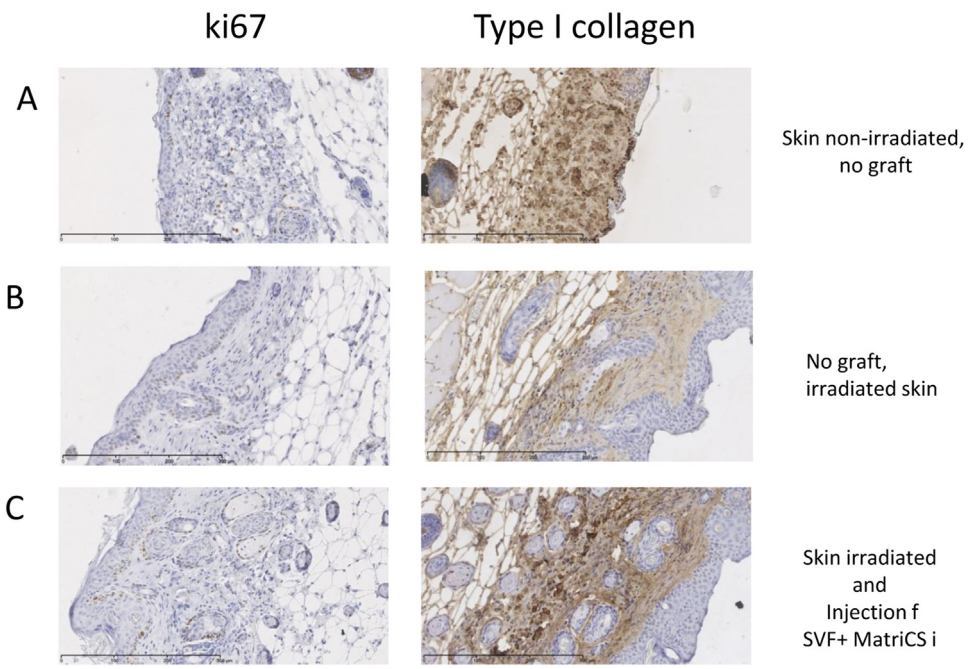

Figure 5. Representative histological staining of skin in UVB-induced wrinkle experiment: (magnification x20). Matrix was exposed (B) or not exposed (A) to cobalt chloride solution. Brown staining can be observed on the section for Ki67, type I collagen. (A). Positive control, normal skin that was not irradiated or treated by injection. (B). Negative control, skin that was irradiated but not treated by injection. (C). Test condition, irradiated skin injected with MatriCS+SVF. (For interpretation of the references to color in this figure legend, the reader is referred to the web version of this article.)

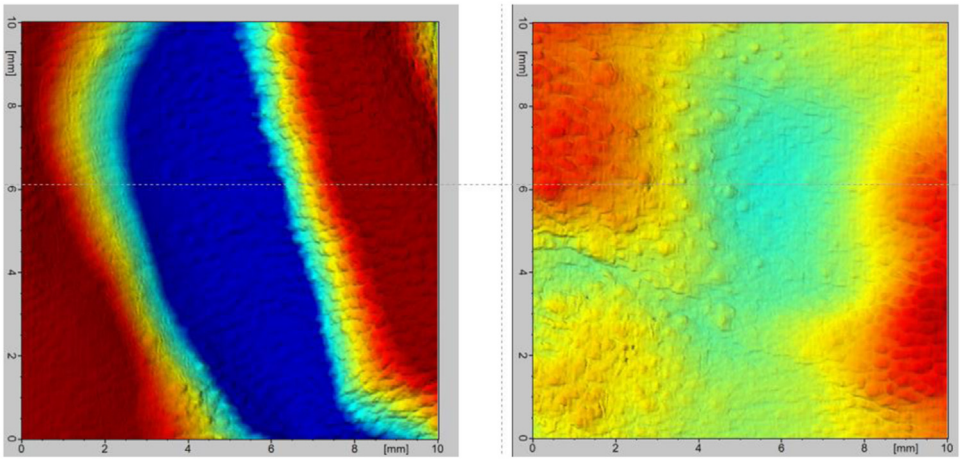

Figure 6. Examples of topographies obtained during the calculation of the macro-relief of a mouse at T0 (left) and at T1 month after injection of SVF+MatriCS (right). The deeper points appear blue, and the shallower points are shown in red. The surface undulations were preserved for calculating the volume. The volume of the wrinkles (mm^3) is in relation to the average plane, and the depth of the wrinkles (µm) corresponds to the difference between the highest and the lowest point on the surface. Each calculated topography has a resolution of 668 × 668 pixels. The size of a pixel being equivalent to 0.015 mm, the analysis region corresponded to an area of 1 cm^2. (For interpretation of the references to color in this figure legend, the reader is referred to the web version of this article.)

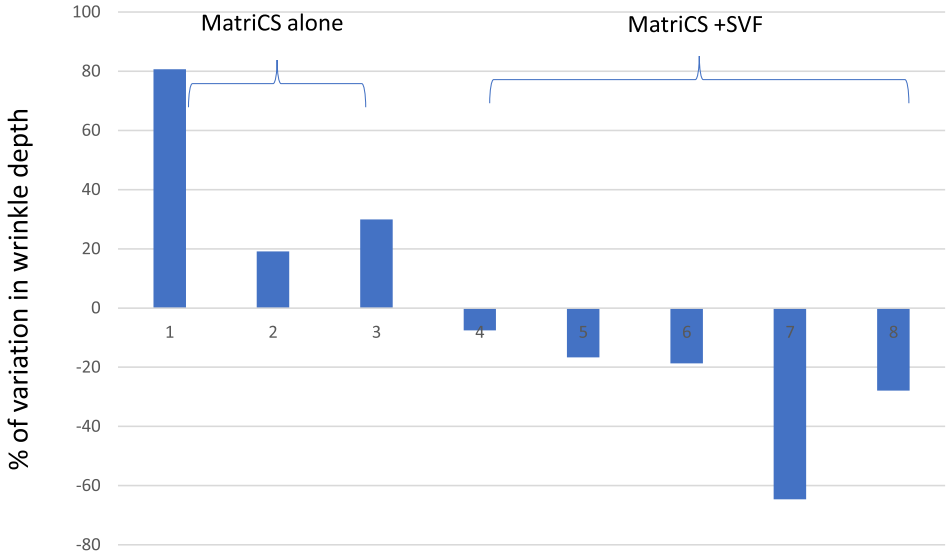

Figure 7. Analysis of wrinkle depth variation: variations in wrinkle depth after subcutaneous injection. The left panel shows the skin injected with MatriCS alone. The right panel shows the skin injected with MatriCS+SVF.

Analysis of wrinkles depth variation was carried out (Figure 7). A negative value indicates that the depth of the wrinkle at the end of the experiment is less than the initial depth of the wrinkle, which indicates the effectiveness of the performed filling. As shown on the left panel of the graph, only replicas from three mice were analyzed since large artifacts disturbed the surface on the other replicas. When MatriCS was injected alone, all values were positive (20 % to 80 %), indicating that the wrinkle were deeper at the end of the experiment than those observed initially. MatriCS alone could not sufficiently fill the wrinkle. The same result was obtained after the injection of SVF alone (data not shown). As shown on the right panel of the graph, when MatriCS + SVF was used, the values were all negative (−8 % to −65 %), indicating that the wrinkle was less deep at the end of the experiment than those observed at the beginning of the experiment. The combination of MatriCS + SVF could fill in the wrinkle lastingly. The values obtained for each condition are representative of inter-individual variability.

According to the literature,[5] the positive effect of cells on fat graft survival is supported by ADSCs. To study this hypothesis using MatriCS, subcutaneous injection of GFP-ADSCs/MatriCS was performed. GFP-ADSCs (1 or 5 × 10^6 cells) were tested to mimic the inter-patient variability in term of cell numbers and their behavior during proliferation, differentiation, migration, and self-renewal.

Irrespective of the dose considered, cell behavior was the same. GFP staining was observed only at the site of injection, *i.e.*, in skin compartment. The staining was visible just after the injection (T0) and also 6 weeks post injection (T6). Cells were mainly located in dermal papilla. Small fluorescent vessels were located in dermal papilla, which indicated neovascularization as evidenced using GFP-ADSC (Figure 8A and B). No GFP staining was observed, at T6, in other organs (lungs, spleen, liver, and kidneys; data not shown). Figure 8C shows the benefit of cobalt chloride conditioning, which was observed as an increase in GFP staining at the skin level in MatriCS compared to that of the unconditioned matrix.

Discussion

For a long time, adipose tissue was perceived as a passive reservoir for energy storage.[19] Nowadays, it is being considered as a complex and highly active metabolic and endocrine organ. Composed

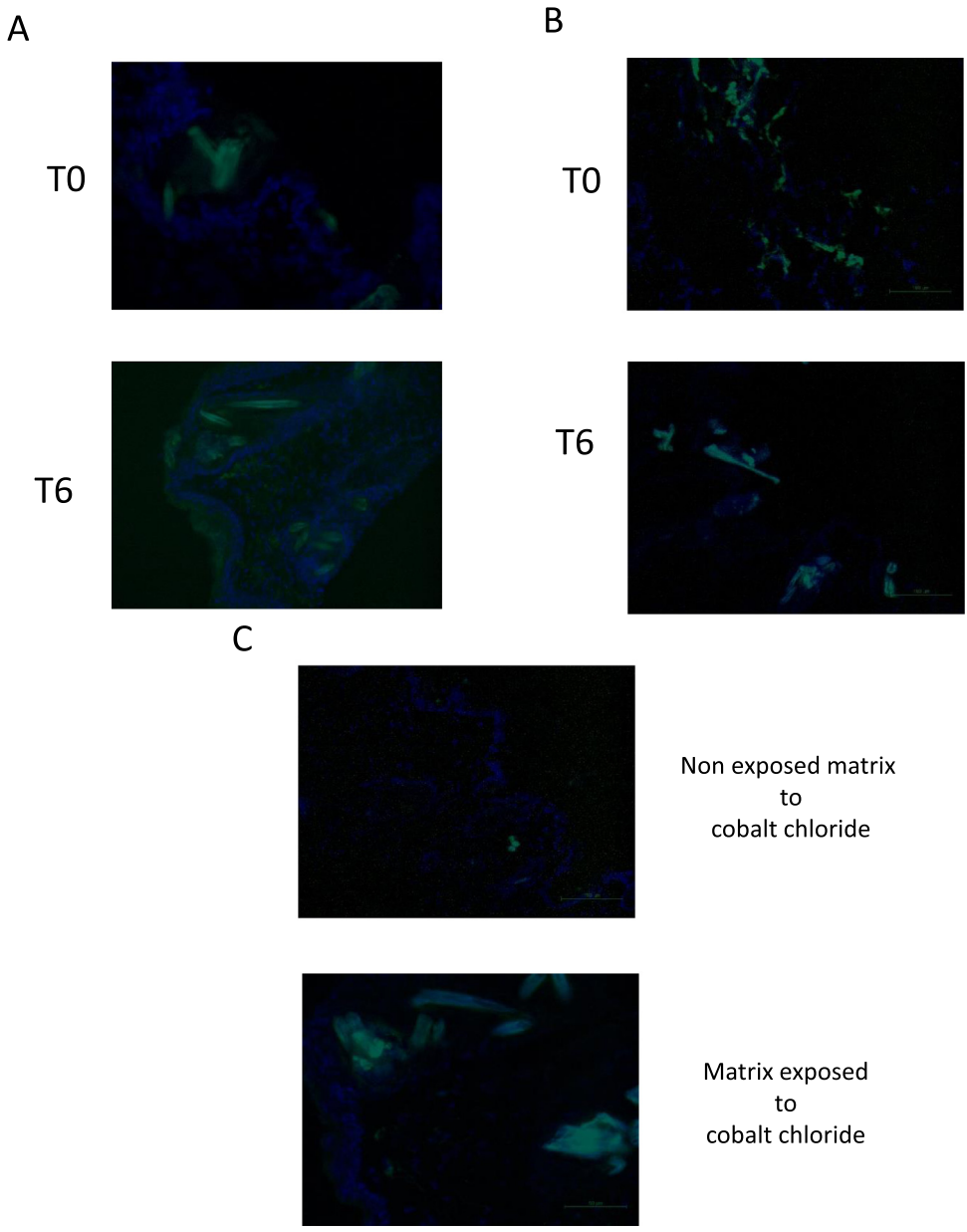

Figure 8. Immunostaining of GFP-ADSCs and local behavior dose (magnification x20) (A). Immunostaining at the site of injection (skin compartment), at T0 and 6 weeks post injection (T6) at low dose (1 M). (B). Immunostaining at the site of injection (skin compartment), at T0 and 6 weeks post injection (T6) at high dose (5 M). (C) Immunostaining of GFP-ADSCs at 6 weeks post injection depending on the cobalt exposure of the matrix.

of connective tissue, nervous tissue, micro vessels, adipocytes, and SVF cells (ADSCs, endothelial progenitors, and immune cells), adipose tissue functions as an integrated unit.[19] Cells included in the adipose tissue are capable of secreting various paracrine factors involved in cell adhesion, proliferation, migration, and differentiation.[19,20]

Several medical devices that use enzymatic or mechanical procedures to isolate stem cells or SVF exist in the market. Each option has its advantages and limitations, but it is well described that the rate of stem cells recovery is lower after mechanical than after an enzymatic procedures.[21] Therefore, enzymatic extraction was chosen for AmeaCell®.

SVF constitutes a highly heterogeneous population. Stem and progenitor cells, including ADSCs in the adipose tissue, usually amount to 30 % of the entire cell population.[22] These cells have been characterized for their specific mesenchymal-associated markers, as expressed in ADSCs after the process.[22] Other lineages present in the SVF are endothelial cells (10–20 %), granulocytes (10–15 %), monocytes/macrophages (5–15 %), lymphocytes (10–15 %), pericytes (1 %), and hematopoietic stem cells.[23] SVF cells contribute to the increased communication between cells and their environment than ADSCs alone. This explains why SVF was used by SYMBIOKEN

SYMBIOKEN developed an innovative and unique process to obtain a pre-conditioned matrix associated with SVF to provide long-lasting effect. After digestion of adipose tissue, the matrix is partially decellularized, and pre-conditioned with cobalt chloride to enhance hypoxia.[24] At the end of the procedure, a part of cobalt is transferred to MatriCS (19–48 µg *vs* initial 174 µg) allowing hypoxia maintenance that will improve SVF cell adhesion, survival, and differentiation,[25,36] when SVF and MatriCS are injected together to the injection site.

Hypoxia of the matrix achieved using the cobalt chloride solution exhibits numerous benefits. It is well documented that hypoxia acts on the cell compartment and extracellular matrix (ECM) composition. Composed of various elements ensuring tissue architecture, the ECM includes structural proteins, such as collagens, and various classes of adhesion proteins, such as fibronectin, laminin, elastin, and proteoglycans.[20] The molecular and structural integrity of MatriCS were evidenced using physicochemical characterization (FTIR-ATR and DSC). Histological studies of MatriCS showed that the expression of collagens (I and IV) was not modified; however, a decrease in laminin expression was observed. Changes in the ECM can trigger a signaling pathway through integrins to intracellular microtubule cytoskeleton and actin filaments leading to the modulation of cell morphology and movements.[27] This laminin decrease can act on the cells that are retained inside MatriCS and also on SVF cells that are added at the end of the process. Laminin is a noncollagen protein constitutive of the ECM, and by binding to the integrins, it contributes to the stimulation of migration of different cell types. For example, laminin-511, is a potent adhesive and pro-migratory substrate for several normal and tumoral cell lines *in vitro*.[28] In our study, laminin decrease induced less interactions with cell receptors leading to less cell migration. The nonmodulation of collagen expression led the cells to adhere to MatriCS, which could also explain why GFP-ADSCs remained at the site of injection irrespective of the cell dosage used. By decreasing the migration of cell, differentiation is favored as demonstrated in this study, and GFP-ADSCs differentiate into cells of dermal papillae and capillaries. This suggests that the hypoxia preconditioning of MatriCS has a positive impact on the ECM composition, as described in the literature. For example, the upregulation of expression of adhesion molecules of endothelial cells, such as intercellular adhesion molecule-1, vascular cell adhesion molecule-1, and endothelial leukocyte adhesion molecule-1, is mediated via hypoxia induced by cobalt chloride.[29]

Hypoxia is also critical for maintaining the stemness of cells. Hypoxia increases the expression of stem-cell markers and the amount of secreted growth factors, such as hepatocyte growth factor and vascular endothelial growth factor (VEGF), in ADSCs.[30] After culture under hypoxic conditions, ADSCs continue to express mesenchymal-associated markers, such as CD73, CD105, and CD90, while they are negative for hematopoietic-associated markers, including CD14, CD45, CD19, CD34, and HLA-DRDPDQ.[25] Hypoxia acts on VEGF by increasing its release, which leads to enhanced vascularization with significant vessel length.[31] These results suggest that the increase in proliferation and vascularization observed in our study can be due to the increase in VEGF release. This is in accordance with the results of our animal experiments, where GFP-ADSCs were found to be more abundant when MatriC + SVF were used in combination compared to that of nonconditioned ma-

trix combined with cells. Expression of GFP is associated with cell proliferation. The hypoxia exposure to the different cell types can modulate their behavior. For example, hypoxia can lead the M1 macrophages to differentiate into M2-like phenotype[32] that are useful for rejuvenation processes by suppressing inflammation, contributing to tissue repair, remodeling, and angiogenesis. Furthermore, M2 macrophages, under the action of SVF, can enhance angiogenesis in adipose transplantation by acting as an angiogenic signal source and promoting cell migration.[32,33] It was reported that the ADSCs in the SVF increased immunoregulatory activity and also blocked the cytotoxic activities of CD8 cells.[34] A recently discovered CD49d+CXCR4highVEGFR1high population of neutrophils was found to specifically migrate to sites of hypoxia and enhance angiogenesis.[35] Moreover, SVF cells increased immunological tolerance by promoting the proliferation of inhibitory macrophages and T regulatory cells and by decreasing ongoing inflammation.[36] Shilts et al. have described that despite arrays of cell-surface proteins organizing immune cells into interconnected cellular communities, linking cells through physical interactions is beneficial for signaling, communication, and structural adhesion.[37] This additional property of immune cells can aid in SVF cells retention at the site of injection.

All these studies and our results indicate that SVF and MatriCS have a potential biomedical impact. A hypoxic conditioning of the matrix combined with SVF can promote long-term wrinkle filling and skin rejuvenation.[26] Our results corroborate those in literature, because the cells in the SVF display mesenchymal stem-cell markers and have a multi-differentiation potential *in vitro* and *in vivo.* Injection of SVF containing ADSCs in combination with MatriCS has demonstrated antiwrinkle effect and safety of this procedure since the stem cells differentiate into cell types present at the injection site.[13] Injection of ADSCs and its secretory factors are effective in producing the antiwrinkle effect, as it is mainly mediated by reducing UVB-induced apoptosis and stimulation of collagen synthesis by human dermal fibroblasts.[13] Koellensperger et al. have demonstrated that ADSCs injected intracutaneously, remain at the site of the injection,[38] survive *in vivo,* and partly differentiate into the cell type required at the injection site led by the new microenvironment.

The use of MatriCS + SVF allows a true cross-talk between them. Individually, each component did not exhibit satisfactory performance as a durable filling. The addition of SVF improved MatriCS volume stability over time and reduced the degradation. Owing to the cobalt chloride preconditioning, MatriCS composition acts as a true scaffold for these cells. MatriCS promotes mechanical support, cell shape/function stability, and transport of chemical signals. In turn, the different cell types in the SVF fraction remain at the site of injection and maintain the MatriCS through their secretions, leading to the survival of the graft and rejuvenation of the skin.

A clinical trial, using the AmeaCell device, focusing on this application would be interesting to conduct to confirm the *in vitro* and *in vivo* results obtained in this study.

Declaration of Competing Interest

None declared.

Acknowledgments

We would like to thank Dr Bravi Serge (Department of Aesthetic and Plastic Surgery, Clinique des Cèdres, Cornebarrieu, France) and Dr Laurent Soubirac (Department of Aesthetic and Plastic Surgery, Medipole, Toulouse, France) for supplying liposuction samples. We also thank Eddy Magdeleine for his contribution to the study (Icelltis company)

Funding

SYMBIOKEN.

Ethical approval

The research protocol for animal studies was approved by the local Ethical Committee (US006/CREFRE Ethics committee).

References

1. Bonta M, Daina L, Muțiu G. The process of ageing reflected by histological changes in the skin. *Rom J Morphol Embryol*. 2013;54(Suppl):797–804.
2. ISAPS global survey 2020
3. Gold MH. Use of hyaluronic acid fillers for the treatment of the aging face. *Clin Interv Aging*. 2007;2:369–376.
4. Coleman SR. Structural fat grafts: The ideal filler? *Clin Plast Surg*. 2001;28:111–119.
5. Yoshimura K, Sato K, Aoi N, et al. Cell-assisted lipotransfer for cosmetic breast augmentation: Supportive use of adipose-derived stem/stromal cells. *Aesth Plast Surg*. 2020;44:1258–1265.
6. Vyas KS, Vasconez HC, Morrison S, et al. Fat graft enrichment strategies: A systematic review. *Plast Reconstr Surg*. 2020;145:827–841.
7. Hong KY. Fat grafts enriched with adipose-derived stem cells. *Arch Craniofac Surg*. 2020;21:211–218.
8. Yin Y, Li J, Li Q, Zhang A, Jin P. Autologous fat graft assisted by stromal vascular fraction improves facial skin quality: A randomized controlled trial. *J Plast Reconstr Aesthet Surg*. 2020;73:1166–1173.
9. Chen J, Lin Y, Jiang H. Fat graft enrichment strategies: A systematic review. *Plast Reconstr Surg*. 2020;146:832 e.
10. Han S, Sun HM, Hwang KC, Kim SW. Adipose-derived stromal vascular fraction cells: Update on clinical utility and efficacy. *Crit Rev Eukaryot Gene Expr*. 2015;25:145–152.
11. Chung HM, Won CH, Sung JH. Responses of adipose-derived stem cells during hypoxia: Enhanced skin-regenerative potential. *Expert Opin Biol Ther*. 2009;9:1499–1508.
12. Tang R, Samouillan V, Dandurand J, et al. Identification of ageing biomarkers in human dermis biopsies by thermal analysis (DSC) combined with Fourier transform infrared spectroscopy (FTIR/ATR). *Skin Res Technol*. 2017;23:573–580.
13. Kim WS, Park BS, Park SH, Kim HK, Sung JH. Antiwrinkle effect of adipose-derived stem cell: Activation of dermal fibroblast by secretory factors. *J Dermatol Sci*. 2009;53:96–102.
14. Miles CA, Burjanadze TV, Bailey AJ. The kinetics of the thermal denaturation of collagen in unrestrained rat tail tendon determined by differential scanning calorimetry. *J Mol Biol*. 1995;245:437–446.
15. Roche S, Delorme B, Oostendorp RA, et al. Comparative proteomic analysis of human mesenchymal and embryonic stem cells: Towards the definition of a mesenchymal stem cell proteomic signature. *Proteomics*. 2009;9:223–232.
16. Sasaki K, Mitsumoto M, Nishioka T, Irie M. Differential scanning calorimetry of porcine adipose tissues. *Meat Sci*. 2006;72:789–792.
17. Berlin E, Sainz E. Fluorescence polarization order parameters and phase transitions in lipids and lipoproteins. *Biochim Biophys Acta*. 1984;794:49–55.
18. Valorani MG, Montelatici E, Germani A, et al. Pre-culturing human adipose tissue mesenchymal stem cells under hypoxia increases their adipogenic and osteogenic differentiation potentials. *Cell Prolif*. 2012;45:225–238.
19. Kershaw EE, Flier JS. Adipose tissue as an endocrine organ. *J Clin Endocrinol Metab*. 2004;89:2548–2556.
20. Chun SY, Lim JO, Lee EH, et al. Preparation and characterization of human adipose tissue-derived extracellular matrix, growth factors, and stem cells: A concise review. *Tissue Eng Regen Med*. 2019;16:385–393.
21. Aronowitz JA, Lockhart RA, Hakakian CS. Mechanical *versus* enzymatic isolation of stromal vascular fraction cells from adipose tissue. *Springerplus*. 2015;4:713.
22. Fraser JK, Zhu M, Wulur I, Alfonso Z. Adipose-derived stem cells. *Methods Mol Biol*. 2008;449:59–67.
23. Zimmerlin L, Donnenberg VS, Pfeifer ME, et al. Stromal vascular progenitors in adult human adipose tissue. *Cytometry A*. 2010;77:22–30.
24. Muñoz-Sánchez J, Chánez-Cárdenas ME. The use of cobalt chloride as a chemical hypoxia model. *J Appl Toxicol*. 2019;39:556–570.
25. Choi JR, Yong KW, Wan Safwani WKZ. Effect of hypoxia on human adipose-derived mesenchymal stem cells and its potential clinical applications. *Cell Mol Life Sci*. 2017;74:2587–2600.
26. Wan X, Xie MK, Xu H, et al. Hypoxia-preconditioned adipose-derived stem cells combined with scaffold promote urethral reconstruction by upregulation of angiogenesis and glycolysis. *Stem Cell Res Ther*. 2020;11:535.
27. Hagiwara M, Maruyama H, Akiyama M, Koh I, Arai F. Weakening of resistance force by cell- ECM interactions regulate cell migration directionality and pattern formation. *Commun Biol*. 2021;4:808.
28. Pouliot N, Kusuma N. Laminin-511: A multi-functional adhesion protein regulating cell migration, tumor invasion and metastasis. *Cell Adh Migr*. 2013;7:142–149.
29. Goebeler M, Meinardus-Hager G, Roth J, Goerdt S, Sorg C. Nickel chloride and cobalt chloride, two common contact sensitizers, directly induce expression of intercellular adhesion molecule-1 (ICAM-1), vascular cell adhesion molecule-1 (VCAM-1), and endothelial leukocyte adhesion molecule (ELAM-1) by endothelial cells. *J Invest Dermatol*. 1993;100:759–765.
30. Yamamoto Y, Fujita M, Tanaka Y, et al. Low oxygen tension enhances proliferation and maintains stemness of adipose tissue-derived stromal cells. *Biores Open Access*. 2013;2:199–205.
31. Mytsyk M, Cerino G, Reid G, et al. Long-term severe *in vitro* hypoxia exposure enhances the vascularization potential of human adipose tissue-derived stromal vascular fraction cell engineered tissues. *Int J Mol Sci*. 2021;22:7920.
32. He Z, Zhang S. Tumor-associated macrophages and their functional transformation in the hypoxic tumor microenvironment. *Front Immunol*. 2021;16:1274–1305.
33. Shapouri-Moghaddam A, Mohammadian S, Vazini H, et al. Macrophage plasticity, polarization, and function in health and disease. *J Cell Physiol*. 2018;233:6425–6440.
34. McIntosh K, Zvonic S, Garrett S, et al. The immunogenicity of human adipose-derived cells: Temporal changes *in vitro*. *Stem Cells*. 2006;24:1246–1253.

35. Campbell EL. Hypoxia-recruited angiogenic neutrophils. *Blood*. 2015;126:1972–1973.
36. Roemeling-van Rhijn M, Mensah FK, Korevaar SS, et al. Effects of hypoxia on the immunomodulatory properties of adipose tissue-derived mesenchymal stem cells. *Front Immunol*. 2013;4:203.
37. Shilts J, Severin Y, Galaway F, et al. A physical wiring diagram for the human immune system. *Nature*. 2022;608:397–404.
38. Koellensperger E, Lampe K, Beierfuss A, et al. Intracutaneously injected human adipose tissue-derived stem cells in a mouse model stay at the site of injection. *J Plast Reconstr Aesthet Surg*. 2014;67:844–850.
39. Rehman I. *Vibrational Spectroscopy for Tissue Analysis*. CRC Press; 2019.
40. Staniszewska E, Malek K, Baranska M. Rapid approach to analyze biochemical variation in rat organs by ATR FTIR spectroscopy. *Spectrochim Acta A Mol Biomol Spectrosc*. 2014;118:981–986.